07

The electro-thermo-optical characteristics and limiting energy capabilities of high-power deep ultraviolet light emitting diodes ($\lambda \approx 270\,\text{nm}$)

© A.L. Zakgeim[1], A.E. Ivanov[1], A.E. Chernyakov[1,2]

[1] Submicron Heterostructures for Microelectronics, Research & Engineering Center, RAS, Saint-Petersburg, Russia
[2] St. Petersburg State Electrotechnical University „LETI", St. Petersburg, Russia
E-mail: zakgeim@mail.ioffe.ru

Received February 1, 2023
Revised February 22, 2023
Accepted February 28, 2023

The current and temperature dependences of the electrical, power and spectral characteristics of high-power deep-UV LEDs ($\lambda \approx 270\,\text{nm}$) have been studied. The main parameters of LED (internal quantum efficiency and light extraction efficiency) which determine output power capacity of the UV LED have been calculated using the *ABC*-model. The influence of current distribution, electrical losses and thermal resistance as factors limiting the energy capabilities was estimated.

Keywords: AlGaN, UV LED, quantum efficiency, light extraction efficiency, temperature dependence, *ABC*-model.

DOI: 10.21883/TPL.2023.05.56018.19519

During the recent decade, significant efforts have been undertaken to create AlGaN-based deep-UV LEDs (UV-C, 200−280 nm). The interest for such emitters is first of all associated with the bactericidal effect of the short-wave ($\lambda < 280\,\text{nm}$) UV radiation and, hence, with their application for sterilizing water, air, etc. [1]. Despite the performed large-scale investigations, the UV LED power parameters, namely, optical power and efficiency factor, still remain much lower than those of the structurally-related AlInGaN LEDs of the visible range ($\lambda = 450{-}490\,\text{nm}$) [2,3].

Revealing of factors playing the main role in restricting the UV LED power capabilities is of great scientific and practical interest. Generally, they may be subdivided into „physical"ones governed by transporting charge carriers into the active region (AR) and their subsequent recombination, and „design"ones determined by the emitting chip design characteristics, namely, by the ability to ensure uniform current distribution, low Joule losses, and efficient radiation extraction and heat removal. The most informative technique for distinguishing and estimating the mentioned factors is experimental investigation of the current and temperature dependences of the electrical, power and spectral LED characteristics; this is just the subject of this study.

The study was concerned with high-power UV LEDs 4550 Mil Bare Chip (Bolb Inc., USA) based on AlGaN heterostructures and having radiation wavelength $\lambda_{peak} \approx 270\,\text{nm}$. To generate such a radiation, a heterostructure is necessary with the AR band gap $E_g \approx 4.5\,\text{eV}$, which corresponds to the quantum well composition $Al_{0.4}Ga_{0.6}N$. The emitting chip $1250 \times 1125\,\mu\text{m}$ in size (total area $S = 1.4\,\text{mm}^2$, active area beneath the *p*-contact $S_{act} = 0.75\,\text{mm}^2$) had the „flip-chip"design with the distributed multilevel system of *p*- and *n*-contacts on the rear side which is most efficient in view of light extraction and heat removal [4]. To ensure current distribution, the interdigitated geometry of contacts was used, in which the main-area *p*-contact was surrounded by a „fork-like" *n*-contact.

Fig. 1, *a* presents a photograph of the emitting chip from the rear („contact") side; Fig. 1, *b* demonstrates the chip photograph from the face emitting side at the operating current $I = 350\,\text{mA}$ in the IR-thermal-imaging microscope. The temperature uniformity over the emitting area (the light spots are associated not with heating but with emission abilities of different elements) evidences for the uniformity of the current distribution and, hence, for the possibility of using mean current density J. Thermal resistance *p*−*n*-junction−mounting plane is $R_{th} \approx 10\,\text{K/W}$ [5].

The UV LED power and spectral characteristics at room temperature and moderate currents were measured in the continuous mode at facility OL770-LEDUV/VIS High-speed LED Test and Measurement System. At high currents, the pulsed mode ($\tau = 100{-}300\,\text{ns}$, $F = 100\,\text{Hz}$) was used, which was provided by generator Agillent 8114A with amplifier PicoLASLDP-V80-100V3.3. The optical signal was detected by a fast-response photoreceiver THORLABS DET02AFC and oscilloscope Tektronix TDS3044. The temperature range was supported by cryostat Janis CCS-450 with an optical window.

The UV LED output power capacity was analyzed based on general expressions for external quantum efficiency η_{EQE} and efficiency factor (wall-plug-efficiency — WPE) [6]:

$$\eta_{\text{EQE}} = \eta_{inj}\eta_{\text{IQE}}\eta_{ext}, \tag{1}$$

$$\text{WPE} = \frac{P_{opt}}{IU} = \frac{\eta_{\text{EQE}} I h\nu/q}{IU} = \eta_{\text{EQE}}\frac{h\nu}{qU} = \eta_{\text{EQE}}\eta_{elect}. \tag{2}$$

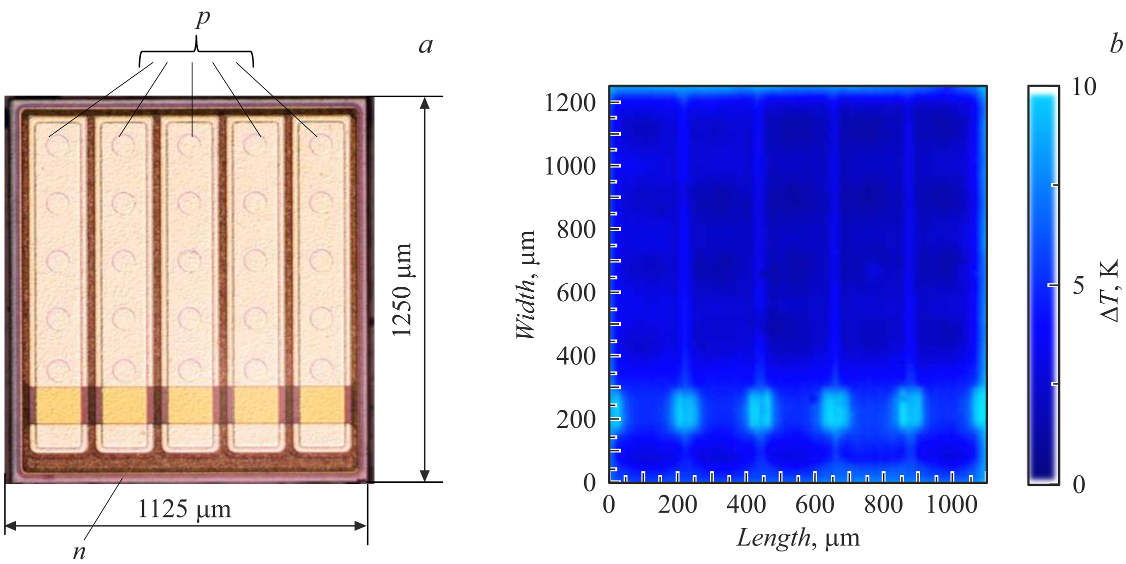

Figure 1. Photos of the emitting „flip-chip“ crystal from the side of the contact group (*a*) and from the side of the emitting surface at operating current $I = 350$ mA in the IR-thermal-imaging microscope (*b*).

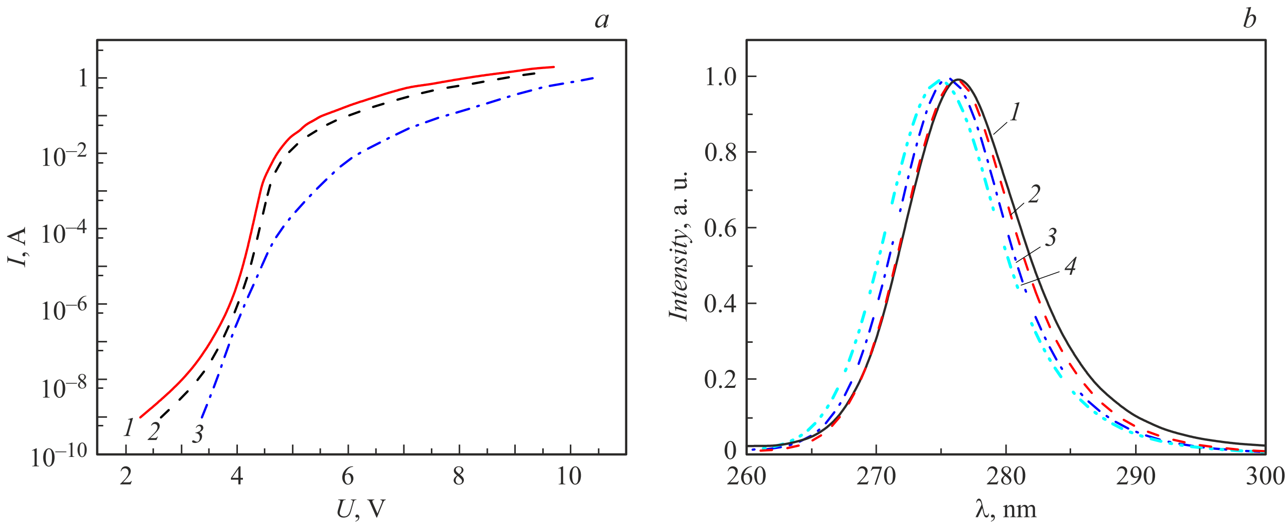

Figure 2. *a* — semi-logarithmic IV characteristics for the temperatures of 353 (*1*), 293 (*2*) and 203 K (*3*); *b* — normalized emission spectra for the current densities of 5 (*1*), 50 (*2*), 500 (*3*) and 2500 A/cm^2 (*4*) at $T = 293$ K.

Here η_{inj} is the injection coefficient, η_{IQE} is the internal quantum efficiency of radiation, η_{ext} is the radiation extraction coefficient, P_{opt} is the output optical power, $h\nu$ is the radiation photon energy, q is the electron charge, I and U are the LED current and voltage; electrical efficiency η_{elect} accounts for the magnitude of exceedance of the energy spent on the electron injection into AR over the energy of the irradiated light photon energy.

Fig. 2, *a* presents a set of UV LED IV characteristics obtained at the temperatures of 200–350 K. In the current range of $I = 10^{-9}$–10^{-2} A ($J = 10^{-7}$–1 A/cm^2), the IV characteristic was measured continuously; further, at $I = 10^{-2}$–$2 \cdot 10^2$ A ($J = 1$–$2.5 \cdot 10^3$ A/cm^2), the measurements were performed in the pulsed mode. Three characteristic regions of the diode characteristic are observed. Below the voltage corresponding to the beginning of the p–n junction opening ($U_f \approx 3.5$ V at $T = 293$ K), the leakage current dominates; further, in the voltage range corresponding to the p–n junction opening ($U_f = 3.5$–4.5 V), the IV characteristic gets the Shockley form

$$I = I_s \exp\left(\frac{qU_f}{\gamma kT}\right), \quad (3)$$

where I_s is the saturation current, q is the electron charge, γ is the ideality factor, k is the Boltzmann constant. From the slope of the IV characteristic exponential section, obtain $\gamma \approx 2.65$ which is close to $\gamma \approx 2.4$ characteristic of high-efficient blue InGaN LEDs and may be regarded as an

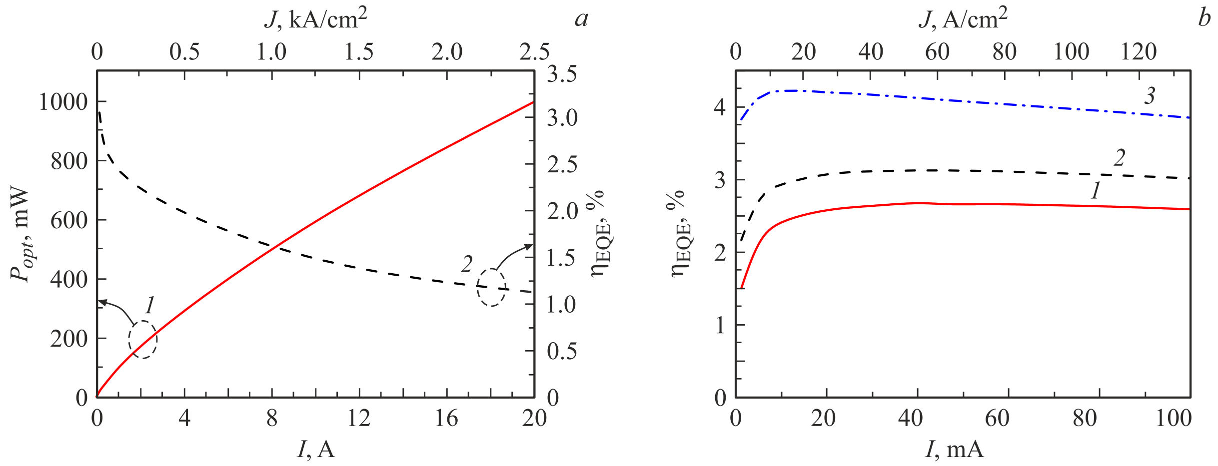

Figure 3. *a* — dependences of P_{opt} (1) and η_{EQE} (2) on current in a wide range of currents (10^{-3}–20 A) at 293 K; *b* — current dependence of η_{EQE} for the temperatures of 353 (1), 293 (2) and 203 K (3).

evidence of acceptability of the injection component of the current. At lower temperatures ($T < 250$ K), the ideality factor increases to $\gamma \approx 4-5$, which stems from the effect of hole „freezing-out" that is, reduction of their equilibrium concentration in the p-region, and also from enhancement of electron leakage and decrease in η_{inj} [7]. After the $p-n$ junction opening ($U_f > 4.5$ V), IV characteristic is determined by an in-series resistance that may be regarded as quite small ($R_s \approx 1\,\Omega$). Thus, the UV LED electrical characteristics seem not crucial in view of its power parameters.

Fig. 2, *b* demonstrates the UV LED spectral characteristics in the current density range covering approximately three orders of magnitude: $J \approx 5-2500$ A/cm^2. Based on them, the following can be noticed:

— the short-wave shift of the spectrum maximum caused by the current increase by three orders of magnitude is only $\Delta\lambda_{peak} \approx 1.5-2$ nm, while the spectrum full width at half maximum (FWHM) remains stable and does not exceed FWHM $\approx 10-12$ nm; these values are essentially lower than in the case of blue AlInGaN light-emitting diodes ($\Delta\lambda_{peak} \approx 25$ nm and FWHM ≈ 32 nm) and evidence for the absence of considerable spontaneous AR polarization and quantum-dimensional Stark effect;

— the absence of the λ_{peak} long-wave shift and constancy of the slope of the short-wave spectrum shoulder versus the radiation energy allow assuming that in the used measurement mode the AR temperature is independent of current (without self-heating).

Fig. 3 presents the main power characteristics of LEDs: current dependences of P_{opt} and η_{EQE}. Fig. 3, *a* presents the dependences in a wide range up to $I = 20$ A ($J = 2.5$ kA/cm^2) at $T = 293$ K, while Fig. 3, *b* demonstrates only current dependences of η_{EQE} but on an enlarged scale for low and medium currents at different temperatures. As Fig. 3 shows, UV LEDs exhibit a considerable deviation from linearity of the light–current characteristic typical of nitride structures; the deviation takes place due to the η_{EQE} decrease with current („efficiency droop"). The maximal value $\eta_{\text{EQE}}^{\max}$ appeared to be 3.4% at current density $J \approx 5$ A/cm^2; with current density increasing to $J > 2$ kA/cm^2, a decrease in η_{EQE} to $\sim 1\%$ is observed (notice for comparison that $\eta_{\text{EQE}}^{\max} \sim 70\%$ in the case of the best AlInGaN-based blue LEDs having a similar design, while at high currents $\eta_{\text{EQE}} \sim 30\%$). To reveal the sources of such a radical difference in efficiencies of the UV and blue LEDs, let us analyze dependences $\eta_{\text{EQE}} = f(I)$ at different temperatures (Fig. 3, *b*).

Behavior of η_{EQE} in Fig. 3, *b* provides two important conclusions. First, η_{EQE} gradually increases with decreasing temperature, and the $\eta_{\text{EQE}}^{\max}$ position shifts towards lower currents due to reduction of the rate of nonradiative Shokley–Read–Hall recombination. Second, as low temperatures ($T < 230$ K) are reached, it becomes possible to clearly fix the $\eta_{\text{EQE}}^{\max}$ position in the current dependences $\eta_{\text{EQE}} = f(I)$, which allows application of the *ABC*-model for calculating absolute values of η_{IQE} [8]. The *ABC*-model implies that η_{EQE} is defined by competition between three recombination mechanisms:

$$\eta_{\text{EQE}} = \eta_{ext}\eta_{\text{IQE}} = \eta_{ext}\frac{Bn^2}{An + Bn^2 + Cn^3}, \qquad (4)$$

where A, B, C are the coefficients accounting for the mechanisms of nonradiative Shockley–Read–Hall recombination, radiative bimolecular recombination and nonradiative Auger recombination, respectively; n is the injected carrier concentration in AR. Using the known transformations [9] in constructing experimental dependences of the reduced quantum efficiency $\eta_{\text{EQE}}^{\max}/\eta_{\text{EQE}}$ on the sum of roots of reduced powers $(p^{1/2} + p^{-1/2})$, where $p = P_{opt}/P_{opt}^{\max}$, and $P_{opt}^{\max}$ is the optical power at the current corresponding to $\eta_{\text{EQE}}^{\max}$, obtain the expression for determining the recombination parameters

$$\eta_{\text{EQE}}^{\max}/\eta_{\text{EQE}} = \eta_{\text{IQE}}^{\max} + \frac{p^{1/2} + p^{-1/2}}{Q+2}, \tag{5}$$

where $Q = B/(AC)^{1/2}$ is the „quality factor"which is a fundamental LED characteristic. By extrapolating the plot constructed based on (5) to $(p^{1/2} + p^{-1/2}) \to 0$, it is possible to determine $\eta_{\text{IQE}}^{\max}$; taking into account that $\eta_{\text{EQE}} = \eta_{ext}\eta_{\text{IQE}}$ and knowing the calculated $\eta_{\text{IQE}}^{\max}$ and experimental $\eta_{\text{EQE}}^{\max}$, it is possible also to obtain η_{ext}, i.e. to find the main parameters defining the LED energy capabilities.

Appropriate processing of $\eta_{\text{EQE}} = f(J)$ (curve *3* in Fig. 3, *b*) provided the following values: $\eta_{\text{IQE}}^{\max} = 0.85$, $\eta_{ext} = 0.048$. Thus, the efficiency of radiation extraction is less than 5% and is the main factor restricting the UV LED energy capabilities. Assuming that η_{ext} is independent of temperature, let us relate the η_{EQE} decrease to a decrease in η_{IQE} to the values of 0.74 and 0.65 at 293 and 323 K, respectively, i.e. η_{IQE} remains much higher than η_{ext} even at high temperatures.

In summary, it is possible to conclude that, at moderate currents and temperatures of $T = 220-350$ K, η_{IQE} of UV LED ($\lambda \sim 270$ nm) belongs to the range $\eta_{\text{IQE}} \approx 80-65\%$. Low values of $\eta_{\text{EQE}}(\sim 2.5-4.5\%)$ and WPE ($R_s \sim 1\,\Omega$ does not significantly contribute to losses) are caused by the smallness of η_{ext} due to the absence of the effect of light „multipassing" the reason for which is absorption on the contacts. Further improvement of the UV LED energy capabilities may be achieved by increasing the contact reflectivity or by including component parts promoting the light extraction from the chip: Bragg reflectors, microdisk mesa-structure, and the like.

Acknowledgements

The LED parameters were studied at Common Use Center „Hardware components for radiophotonics and nanoelectronics: technology, diagnostics, metrology".

Conflict of interests

The authors declare that they have no conflict of interests.

References

[1] V. Sharma, H. Demir, ACS Photon., **9** (5), 1513 (2022). DOI: 10.1021/acsphotonics.2c00041
[2] Q. Chen, J. Dai, X. Li, Y. Gao, H. Long, Z. Zhang, C. Chen, H. Kuo, IEEE Electron Dev. Lett., **40** (12), 1925 (2019). DOI: 10.1109/LED.2019.2948952
[3] A.L. Zakgeim, A.V. Aladov, A.E. Ivanov, N.A. Talnishnikh, A.E. Chernyakov, Tech. Phys. Lett., **48** (7), 29 (2022). DOI: 10.21883/TPL.2022.07.54033.19182.
[4] D.A. Zakgeim, G.V. Itkinson, M.V. Kukushkin, L.K. Markov, O.V. Osipov, A.S. Pavlyuchenko, I.P. Smirnova, A.E. Chernyakov, D.A. Bauman, Semiconductors, **48** (9), 1254 (2014). DOI: 10.1134/S1063782614090267.
[5] A.L. Zakgeim, A.E. Ivanov, A.E. Chernyakov, v sb. *Radioelektronnaya tekhnika* (UlGTU, Ulyanovsk, 2022), s. 86. (in Russian)
[6] F.E. Schubert, *Light-emitting diodes*, 2nd ed. (Cambridge University Press, Cambridge, 2006). DOI: 10.1017/CBO9780511790546.
[7] A.S. Pavluchenko, I.V. Rozhansky, D.A. Zakheim, Semiconductors, **43** (10), 1351 (2009). DOI: 10.1134/S1063782609100170.
[8] S.Yu. Karpov, Opt. Quant. Electron., **47** (6), 1293 (2015). DOI: 10.1007/s11082-014-0042-9
[9] I. Titkov, S. Karpov, A. Yadav, V. Zerova, M. Zulonas, B. Galler, M. Straßburg, I. Pietzonka, H. Lugauer, E.U. Rafailov, IEEE J. Quant. Electron., **50** (11), 911 (2014). DOI: 10.1109/JQE.2014.2359958

Translated by Solonitsyna Anna